PHYSICAL REVIEW A VOLUME 45, NUMBER 9 1 MAY 1992

Far-infrared self-broadening in methylcyanide: Absorber-perturber resonance

G. Buffa and O. Tarrini
Dipartimento di Fisica dell'Università, Piazza Torricelli 2, I-56126, Pisa, Italy

P. De Natale, M. Inguscio, F. S. Pavone, and M. Prevedelli
Dipartimento di Fisica dell'Università and European Laboratory for Nonlinear Spectrscopy (LENS), Largo Fermi 2, Arcetri, I-50125 Firenze, Italy

K. M. Evenson and L. R. Zink
National Institute for Standards and Technology, 325 Broadway, Boulder, Colorado 80303

G. W. Schwaab
Max-Planck-Institut für Radioastronomie, auf dem Hügel, 69 D-5300 Bonn, Germany

(Received 16 December 1991)

Using tunable far-infrared spectrometers with high-frequency stability and accuracy, we have measured the self-pressure broadening and shift of CH_3CN. We obtained clear evidence of absorber-perturber resonance effects on the collisional line shape. This tests the theoretical model and its possible improvements and also allows us to make broadening and shift predictions for a large class of molecules. Moreover, the resonance effect produces a theoretical temperature dependence of self-broadening that is very different from what is commonly assumed.

PACS number(s): 33.70.Jg, 33.20.Ea

I. INTRODUCTION

Using two similar tunable far-infrared (TFIR) spectrometers (from two different laboratories) with high-frequency stability and accuracy, we have measured the self-induced pressure broadening and shift of CH_3CN for a number of lines with J'', the rotational quantum number for the lower state, ranging from 21 to 68. The collisional line shape of the CH_3CN spectrum has been widely investigated [1–6] in the microwave spectral region where self-broadening and shift and foreign gas broadening of the rotational lines were measured and compared to theoretical calculations for J'' ranging from 0 to 5. Recent advances in the generation of cw TFIR radiation now make possible the measurement of pressure broadening and shift in the 0.5-to-6-THz spectral region [7], where transitions between high rotational levels of CH_3CN occur.

Comparisons with theoretical predictions are particularly attractive for CH_3CN. The dipole-dipole interaction is strong enough to produce a complete loss of coherence in the dipole correlation function for collision impact parameters as large as 2 nm; the relaxation effect of such collisions is therefore easily calculated. For larger impact parameters it is possible to assume classical linear trajectories, as is done in the Anderson-Tsao-Curnutte (ATC) theory [8,9]. We compared measurements with theory and obtained satisfactory agreement. Discrepancies give clear indications on the type of refinements that must be introduced in the theoretical approximations.

Our measurements verify the large effect of absorber-perturber resonance on the collisional relaxation. Indeed, according to the theory, a crucial parameter is energy transferred to translation from the internal energy of the absorber-plus-perturber system. Resonance occurs when the collisional change of the internal energy of the absorbing molecule almost balances that of the perturbing molecule, so that only a small part of the exchanged rotational energy is transferred to translation. Due to resonance effects, the pressure-broadening coefficient exhibits a maximum for J'' values near the most populated level $\bar{J}$; for CH_3CN at room temperature, $\bar{J} \simeq 20$. To be precise, the most populated level is $J=18$, while the thermally averaged value of J is 23. Moreover, the shift coefficient is expected to be positive if $J'' < \bar{J}$ and negative if $J'' > \bar{J}$. Having experimentally verified the reliability of these theoretical predictions, we theoretically derive the dependence of broadening and shift on the molecular constants and rotational quantum numbers for a large class of symmetric top and linear molecules. We also show that the resonance causes the temperature dependence of pressure broadening to be very different in the far-infrared (FIR) region than in the microwave region.

II. EXPERIMENT

We used the TFIR spectrometers at the National Institute for Standards and Technology (NIST) in Boulder, Colorado [10] and at the European Laboratory for Nonlinear Spectroscopy (LENS) in Florence, Italy [11] to produce coherent FIR radiation. Both spectrometers were operated in third-order mode (see Fig. 1): Two frequency-stabilized CO_2 lasers with frequencies ν_I and

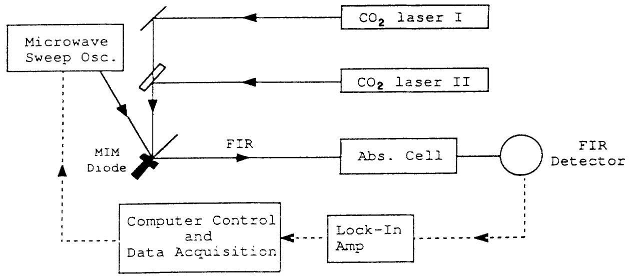

FIG. 1. Schematic diagram of the experimental apparatus.

ν_{II} were mixed with a 0.01-to-20-GHz microwave component ν_μ in a metal-insulator-metal (MIM) point-contact diode to produce upper and lower sideband radiation at the difference frequency

$$\nu_{FIR} = |\nu_I - \nu_{II}| \pm \nu_\mu . \tag{1}$$

The uncertainty of the FIR frequency is given by the quadrature sum of the uncertainties of the single lasers, which amounts to typically 35 kHz. The MIM contact consisted of an electrochemically etched 25-μm-diam tungsten wire contacting a polished cobalt substrate at normal incidence. The cone of the whisker acts as an antenna for the CO_2 laser radiation, whereas the several-millimeter-long whisker acts as a long wire antenna for the FIR. A corner reflector was adjusted to improve the FIR radiation pattern [12]. The beam was reflected by an off-axis parabola and sent through a single-pass Pyrex absorption cell with an inner diameter of 22 mm and high-density polyethylene windows. To prevent line-shape distortions, different cells with lengths from 3 to 84 cm were used, depending on the line strengths.

To reduce standing waves, all optical components were slightly tilted and wedged. In addition, the optical path was modulated by several wavelengths with a moving mirror system. The radiation was detected by a liquid-He-cooled Ge bolometer (NIST) or composite Si bolometer (LENS). We used 300-mW CO_2 laser power and 3-10 mW of microwave power, which typically yielded 10–100 nW of FIR radiation. The FIR radiation was frequency modulated by modulating the CO_2 lasers and phase-sensitivity detected with a lock-in amplifier. The data acquisition on both systems is fully computerized.

The measurements at LENS used sealed absorption cells; when short cells were used, a 0.5-l gas ballast was attached to the cell. The modulation depth ranged from 1.6 to 4.8 MHz and the temperature was 296±2 K. In the NIST measurements the temperature was 302-304 K while a modulation depth of 0.8 MHz and a flowing system were used. Pressures ranged from 0.7 to 133 Pa and were measured to better than 3% with temperature-stabilized, precision capacitance manometers; five to ten pressure points were used to evaluate the broadening and shift parameters of a single line.

A typical example of a measured spectrum is reported in Fig. 2. The fitted curve was generated by use of a nonlinear least-squares-fitting routine provided by Kelly

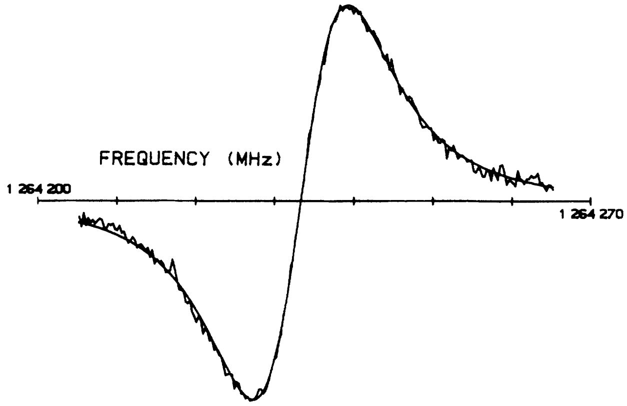

FIG. 2. Experimental and best-fit shape of the rotational $J=69\leftarrow68$, $K=3$ absorption line at 104 Pa.

Chance of the Harvard Smithsonian Center for Astrophysics. Fitting parameters were the transition frequency, the Lorentzian width, the baseline offset, and a multiplicative scaling factor. The line intensity and the Gaussian (Doppler) width were fixed to the calculated values.

The pressure dependence of the fitted Lorentzian widths and line frequencies was used to obtain pressure-broadening and shift parameters. Figure 3 illustrates this

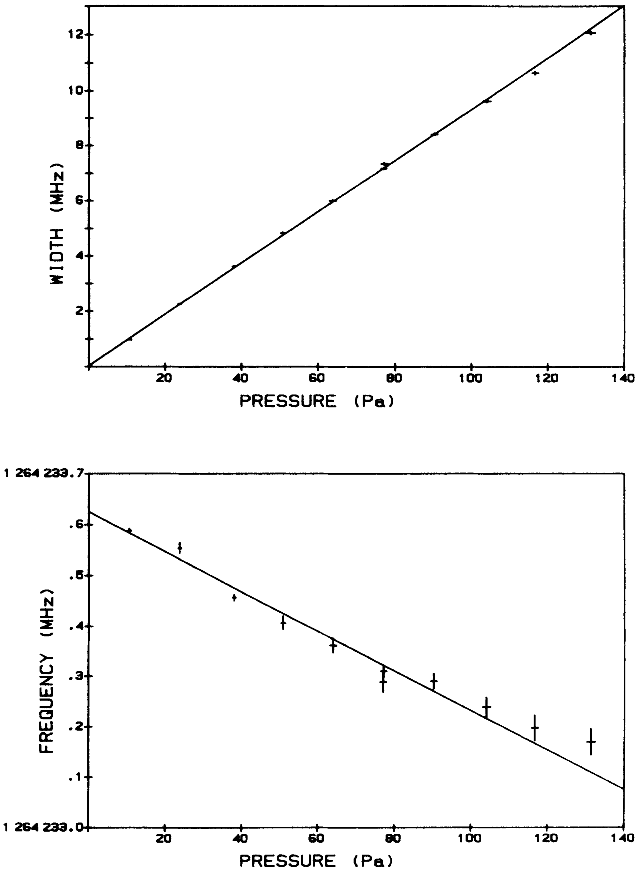

FIG. 3. Pressure dependence of the Lorentzian linewidth and center frequency for the transition $J=69\leftarrow68$, $K=3$.

TABLE I. Measured self-broadening halfwidth at half maximum, shift parameters, and zero-pressure transition frequencies of CH_3CN. Values in parentheses are 2σ uncertainty of the last digits.

Transition		Broadening	Shift	Frequency
J''	K	(kHz/Pa)	(kHz/Pa)	(kHz)
21[a]	3	555(37)		408 520 319(56)
35[a]	3	353(45)		661 496 322(61)
39[a]	3	315(30)		734 808 277(53)
42[b]		209(11)	−8.3(30)	789 759 827(48)
43[b]		203(11)	−7.5(30)	808 068 124(54)
49[a]	3	161(22)		917 830 713(60)
55[b]		114(15)	−6.0(23)	1 027 428 711(60)
56[a]	5	122(11)	−11.3(30)	1 045 366 176(38)
56[a]	8	113(9)	−7.5(38)	1 044 608 225(40)
67[b]		83(15)	−3.8(15)	1 246 053 109(44)
68[a]	3	84(9)	−3.8(8)	1 264 233 624(18)

[a] Measurement performed at LENS.

[b] Measurement performed at NIST. The reported values are a weighted average over different K transitions. The transition frequency is for $K=3$.

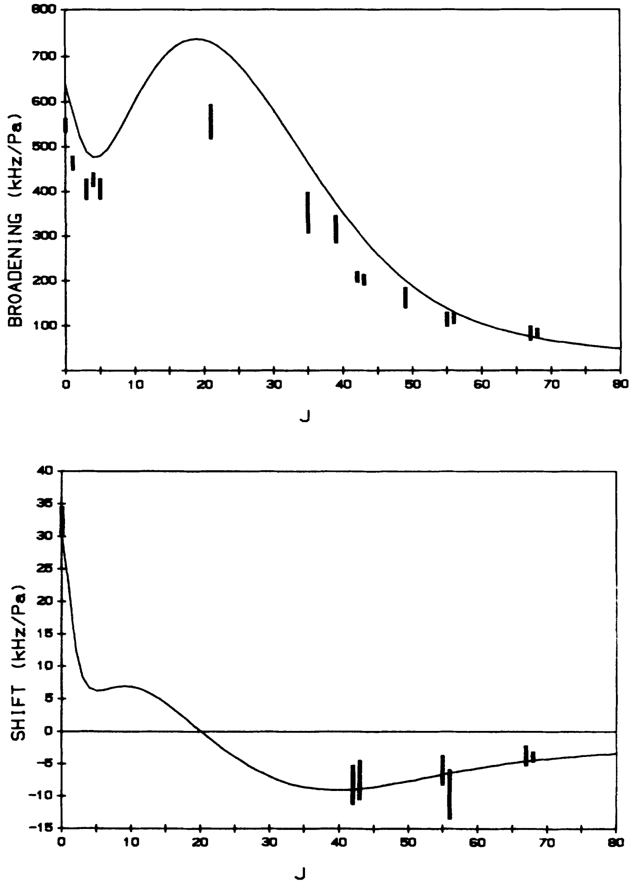

FIG. 4. Comparison between theoretical and experimental J'' dependences of the self-broadening and shift parameters of the rotational transitions of CH_3CN. The FIR measurements are from the present work. References for the microwave measurements are $J''=0$, Refs. [4] and [5] for both broadening and shift; $J''=1$, Ref. [2]; $J''=3$, Ref. [3]; $J''=4$, Ref. [6]; $J''=5$, Ref. [1]. The theoretical curve was calculated for 296 K, $K=0$, and includes dipole-dipole, dipole-quadrupole, and quadrupole-quadrupole interactions.

for the $J''=68$, $K=3$ transition. At 77 Pa we recorded the spectrum at modulation depths of 2.4 and 4.8 MHz, to investigate the modulation broadening.

The experimental results are reported in Table I. Measurements were performed for J'' ranging from 21 to 68. For some lines, the value of the shift coefficient is less than the measurement uncertainty and hence could not be determined. Results obtained in the two different laboratories match very well and are also in agreement with a previous measurement for $J''=43$ [13].

For $J''=42$, 43, 55, and 67 the reported values correspond to a weighted average over K. Indeed, apart from small variations on the order of the experimental error, the broadening and shift measurements show [14] a very weak K dependence, at least for $K \leq 10$. Transitions with higher K values were too weak to be studied. The measured dependences of the broadening and shift on J'' are shown in Fig. 4, which also includes some microwave data [5] for low K/J'' values. The broadening exhibits two maxima, one at $J''=0$ and the other near $J''=20$. The shift is negative for the FIR lines and positive in the microwave region. Figure 4 also reports the calculated curves, which are discussed in Sec. III.

III. THEORY

At low pressures, relaxation is due to binary collisions and the pressure broadening w and shift s can be calculated [15] in the framework of an impact approximation. w and s are linear with the number density n of the gas and they are expressed, respectively, by the real and imaginary parts of a complex relaxation operator M, averaged on all possible collisions:

$$w+is=n\langle M(r,l)\rangle_{r,l}\ , \tag{2}$$

where $\langle\ \rangle_{r,l}$ represents the thermal average on the internal states r of the perturbing molecule and on the angular momentum l of the relative motion. For a line $i \longrightarrow f$, the relaxation operator M can be derived from the scattering matrix $S=1-T$:

$$M(r,l)=\langle i,r,l|T|i,r,l\rangle+\langle f,r,l|T^{\dagger}|f,r,l\rangle-\sum_{r',l'}\langle i,r,l|T|i,r',l'\rangle\langle f,r',l'|T^{\dagger}|f,r,l\rangle \; . \tag{3}$$

The three terms on the right-hand side of Eq. (3) are commonly called two "outer" (initial and final) terms and one "middle" term, bilinear in T.

Since an exact calculation of the scattering matrix is not easily realized, various approximations have been proposed. The most common is the semiclassical approximation, which assumes that the translational motion follows classical mechanics and uses quantum mechanics to describe the influence of the collision on the internal states of the molecules. Hence, Eqs. (2) and (3) take a form in which the translational state is described by the impact parameter b and the relative velocity v:

$$w+is=n\sum_{r}\rho_r\int_0^{\infty}dv\; vf(v)\int_0^{\infty}db\; 2\pi bP(b,v,r) \; , \tag{4}$$

$$P(b,v,r)=\langle i,r|T(b,v)|i,r\rangle+\langle f,r|T^{\dagger}(b,v)|f,r\rangle-\sum_{r'}\langle i,r|T(b,v)|i,r'\rangle\times\langle f,r'|T^{\dagger}(b,v)|f,r\rangle \; , \tag{5}$$

where ρ_r is the population of the level r, $f(v)$ is the Maxwellian velocity distribution, and P is the semiclassical relaxation efficiency function.

The calculation of P is easily realized for weak collisions, that is, for collisions occurring with such large impact parameters that the intermolecular interaction can be considered to be a small perturbation. Furthermore, the effects of strong collisions are easily evaluated, because every coherence is lost. Problems arise, however, in the intermediate range. The existing semiclassical theories differ on this point, but all of them are based on extrapolations of the perturbative calculation for weak collisions.

The lowest-order perturbation expansion of Eq. (5) yields

$$\mathrm{Re}P(b,v,r)=\frac{1}{2\hbar^2}\sum_{r'}\left[\sum_{i'}|\langle i,r|V(\omega_{ii'}+\omega_{rr'})|i',r'\rangle|^2+\sum_{f'}|\langle f,r|V(\omega_{ff'}+\omega_{rr'})|f',r'\rangle|^2-2\langle i,r|V(\omega_{rr'})|i,r'\rangle\langle f,r|V(\omega_{rr'})|f,r'\rangle\right] , \tag{6}$$

and

$$\mathrm{Im}P(b,v,r)=\frac{1}{2\hbar^2}\sum_{r'}\left[\sum_{i'}|\langle i,r|\tilde{V}(\omega_{ii'}+\omega_{rr'})|i',r'\rangle|^2-\sum_{f'}|\langle f,r|\tilde{V}(\omega_{ff'}+\omega_{rr'})|f',r'\rangle|^2\right] , \tag{7}$$

where $\omega_{ab}=(E_b-E_a)/\hbar$ is the energy of the molecular transition $a\rightarrow b$. The function $V(\omega)$ in Eq. (6) is the Fourier transform of the time-dependent collisional interaction $V(t)$, and $\tilde{V}(\omega)$ in Eq. (7) is the Hilbert transform of $V(\omega)$:

$$\tilde{V}(\omega)=\frac{1}{\pi}\mathrm{P}\int_{-\infty}^{\infty}d\omega'\frac{V(\omega')}{\omega-\omega'} \; , \tag{8}$$

where P denotes principal value. The terms inside the parentheses in Eqs. (6) and (7) show that ReP is the sum of an initial, a final, and a middle term, and ImP is the difference of an initial and a final term; the lowest-order shift contribution from the middle term vanishes.

In Eqs. (6) and (7) $\hbar(\omega_{ii'}+\omega_{rr'})$ and $\hbar(\omega_{ff'}+\omega_{rr'})$ are the energy transferred between translation and internal degrees in the collision. P decreases rapidly as the transferred energy increases and this provides reliability for the semiclassical approximation: It is surely inaccurate when the transferred energy is not a small part of the translational energy, but these collisions give a small contribution to P. For the same reason, even if the sums in Eqs. (6) and (7) extend to all the transitions $r\rightarrow r'$ of the perturbing molecule and $i\rightarrow i'$, $f\rightarrow f'$ of the absorbing molecule, vibrational energy changes can usually be excluded because the energy transfer involved is so high that they are negligible. As a consequence, the collisional line-shape parameters of the rovibrational P and R bands are very similar to the ones of the corresponding rotational lines, provided the rotational energy pattern of the excited state is similar to that of the ground state.

We restrict ourselves now to the case of molecules, such as CH_3CN, for which the dipole-dipole interaction is so strong that the contribution of other interactions is small and the ATC assumption of classical linear trajectories is reliable. Indeed, in our case, the broadening cross section $\sigma=\pi r^2=w/n\bar{v}$ is so large that the radius r ranges for the measured lines from 1.1 to 2.9 nm and is always much larger than the kinetic radius.

Under these assumptions, the ω dependence of $V(\omega)$ and $\tilde{V}(\omega)$ is given, respectively, by calculable functions $f_{dd}(k)$ and $\phi_{dd}(k)$ of the dimensionless parameter

$$k=\frac{\omega b}{v}=\frac{\Delta Eb}{\hbar v} \; . \tag{9}$$

The shapes of the dipole-dipole resonance functions $f_{dd}(k)$ and $\phi_{dd}(k)$ are shown in Fig. 5. f_{dd} is an even function of k, is close to 1 for small values of k, and is very rapidly decreasing for $k>2$; when k is large, $f_{dd}(k)\simeq\pi k^3 e^{-2k}$. On the contrary, ϕ_{dd} is odd with k and has a more complicated shape; when k is large, $\phi_{dd}(k)\simeq 9\pi/16k$.

For symmetric top molecules the rotational states are described by the quantum numbers J and K. The dipole selection rules are $\Delta J=0,\pm1$ and $\Delta K=0$, and the states i, i', f, f', r, and r' are labeled J_iK, $J_i'K$, J_fK, $J_f'K$, J_rK_r, and $J_r'K_r$. Hence, for a dipole-dipole interaction and symmetric top molecules, the ATC form of Eqs. (6) and (7) can be written as

$$\mathrm{Re}P=\frac{4\mu^4}{9v^2\hbar^2b^4}\sum_{J_r'}|\langle J_r'K_r|10J_rK_r\rangle|^2\Bigg[\sum_{J_i'}|\langle J_i'K|10J_iK\rangle|^2 f_{dd}(k_{ii'}+k_{rr'})+\sum_{J_f'}|\langle J_f'K|10J_fK\rangle|^2 f_{dd}(k_{ff'}+k_{rr'})$$

$$-2(-1)^{J_i+J_f}W(J_iJ_iJ_fJ_f;11)$$

$$\times\sqrt{(2J_i+1)(2J_f+1)}\langle J_iK|10J_iK\rangle\langle J_fK|10J_fK\rangle f_{dd}(k_{rr'})\Bigg]\,, \tag{10}$$

and

$$\mathrm{Im}P=\frac{4\mu^4}{9v^2\hbar^2b^4}\sum_{J_r'}|\langle J_r'K_r|10J_rK_r\rangle|^2\left[\sum_{J_i'}|\langle J_i'K|10J_iK\rangle|^2\phi_{dd}(k_{ii'}+k_{rr'})+\sum_{J_f'}|\langle J_f'K|10J_fK\rangle|^2\phi_{dd}(k_{ff'}+k_{rr'})\right]\,, \tag{11}$$

where μ is the molecular dipole moment, W is a 6-j Racah coefficient and the arguments k of the resonance functions are given by Eq. (9).

Equations (10) and (11) allow calculations of the pressure broadening and shift, and also yield qualitative insight into their dependence on the J and K quantum numbers and on the molecular constants. We discuss briefly the dependence of the broadening parameter without entering into details for the shift parameter because the shift resonance function has a more complicated shape and because the frequency shift is a sum of many terms with different signs.

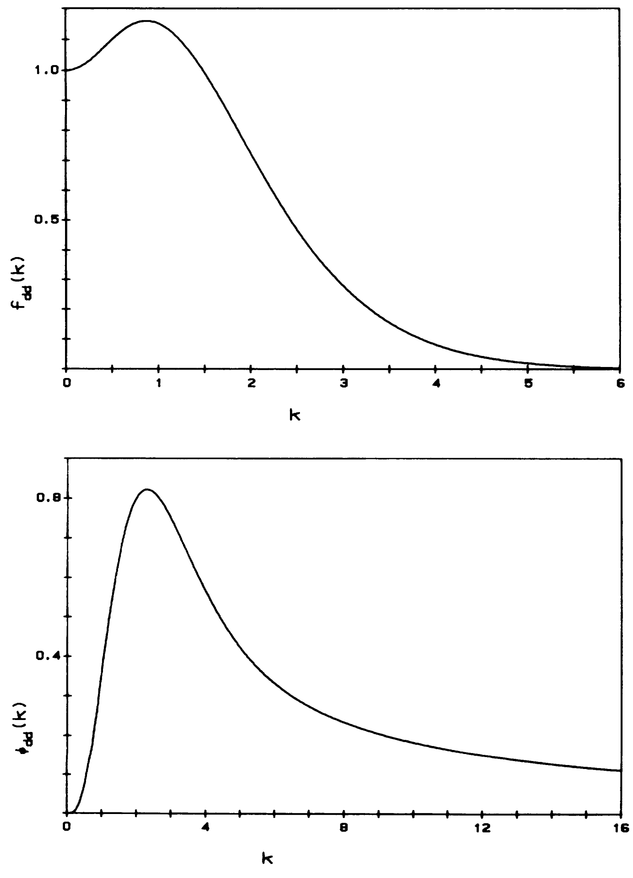

FIG. 5. Shape of the resonance functions $f_{dd}(k)$ and $\phi_{dd}(k)$ occurring in the pressure-broadening and shift calculations, respectively.

Equation (10) and Fig. 5 show that collisional transitions involving k values larger than a few units give a strongly reduced broadening contribution. In order to give an idea of the energy scale in Fig. 5, we remember that for $\mathrm{CH_3CN}$ at the average room-temperature velocity and for a typical b value of 2 nm, $k\simeq0.7\Delta E$, where ΔE is expressed in cm^{-1}. The energy jump is $\Delta E=0$ for the $\Delta J=0$ transitions and $|\Delta E|\simeq2BJ$ for J-changing transitions. For the $\mathrm{CH_3CN}$ molecule $B\simeq0.3\ \mathrm{cm}^{-1}$ and $|k|\simeq0.4J$. As a consequence, for J-changing transitions, k is small only for low J values (approximately $J<5$).

Another remarkable point is that the broadening contribution from the $\Delta J=0$ transitions of the absorber is reduced by a factor of the order $1/J^2$ because the middle term in Eq. (10) almost exactly cancels the two outer (initial and final) terms. Indeed, restricting the sums in Eq. (10) to $\Delta J_i=\Delta J_f=0$, using explicit expressions for the Clebsch-Gordan and Racah coefficients, and because $J_f=J_i+1$ for a rotational line, the expression inside the parentheses on the right-hand side of Eq. (10) becomes

$$\left[\frac{K^2}{J_i(J_i+1)}f_{dd}(k_{rr'})+\frac{K^2}{J_f(J_f+1)}f_{dd}(k_{rr'})\right.$$

$$\left.-\frac{K^2[J_i(J_i+1)+J_f(J_f+1)-2]}{J_i(J_i+1)J_f(J_f+1)}f_{dd}(k_{rr'})\right]$$

$$=\frac{2K^2}{J_i(J_i+1)J_f(J_f+1)}f_{dd}(k_{rr'})\,. \tag{12}$$

On the whole, for lines with high J values, a large broadening contribution can be given only by resonant collisions for which the rotational energy is transferred from one molecule to the other, that is, $k_{rr'} \simeq -k_{ii'}$ (or $k_{rr'} \simeq -k_{ff'}$). The peak at $J=\bar{J}$ in Fig. 4 is due to this type of collision. Indeed, resonant collisions can occur only if $J_i \simeq J_r$ or $J_f \simeq J_r$ and, because of the weighted average on r appearing in Eq. (4), it is clear that the contribution of resonant collisions is enhanced for lines with J near to the most populated value $\bar{J}$. This feature is not restricted to CH_3CN but extends to rotational spectra of all symmetric top or linear molecules whose collisional interaction is mainly dipole-dipole. Indeed, the same effect can be found for self-broadening in the fundamental bands of HF and HCl, despite their much larger B rotational constant. Measurements by Pine and Fried [16] exhibit, for both P and R branches of both molecules, a maximum broadening for $J \simeq \bar{J}$ and a rapid decrease at higher J.

Exceptions to a J dependence of this type can be due to the presence of terms in the molecular Hamiltonian other than rotation, giving rise to different energy patterns and selection rules; an example of this is the inversion Hamiltonian of ammonia, which causes the middle term to disappear from Eq. (6). Also, the trend of the shift parameter, positive for $J<\bar{J}$ and negative for $J>\bar{J}$, extends to other strongly dipolar symmetric top or linear molecules and can be derived from Eq. (11).

For lines with low J values, the contribution of resonant collision is not very important because of the low population of the involved J_r states. However, a large broadening contribution can arise from adiabatic or quasiadiabatic collisions involving small changes in the rotational energy, that is,

$$k_{rr'} \simeq 0 \ , \tag{13}$$

$$k_{ii'} \simeq 0, \quad k_{ff'} \simeq 0 \ . \tag{14}$$

Condition (13) for the perturber is fulfilled only by the $\Delta J_r=0$ transitions and by a small part of the J_r-changing transitions: The fraction of perturbing molecules with $J_r \leq 5$ is only 3% of the total. For the absorber, on the contrary, conditions (14) are fulfilled at low J by both $\Delta J=0$ and J-changing transitions. If J increases, the contribution of J-changing transitions is decreased by the increase of $k_{ii'}$ and $k_{ff'}$, while the contribution of $\Delta J=0$ transitions is decreased by the growing influence of the middle term, as shown by Eq. (12). This explains the peak at $J=0$, which is due to adiabatic or almost adiabatic collisions.

Different from the peak at $J \simeq \bar{J}$, the peak at $J=0$ does not extend to all strongly dipolar symmetric top and linear molecules. In order to stress this fact, we display in Fig. 6 the J dependence of self-pressure-broadening and shift parameters for the $K=0$ lines of some hypothetical symmetric top molecules having the same mass, dipole moment, and B rotational constant as CH_3CN, but with different C rotational constant. The larger C is, the less populated the high K_r/J_r states are, and consequently the less effective the $\Delta J_r=0$ transitions are, having in Eq. (10) a Clebsch-Gordan coefficient equal to $K_r^2/J_r(J_r+1)$. For linear molecules, $K_r=0$, and the $\Delta J_r=0$ transitions give no contribution. We considered C ranging from $B/2$, corresponding to an extremely oblate symmetric top molecule, to ∞, corresponding to a linear molecule. The cases of a spherical top ($C=B$) and the true CH_3CN value ($C=4.94$ cm^{-1}) are included. Figure 6 shows that for both the broadening and shift coefficients, the peak at $J=0$ is due to adiabatic transitions. The peak is increased for decreasing values of C and is absent for linear molecules, as confirmed by the measurements [16] on HF and HCl. On the contrary, the minor changes at higher J are due to the resonance: $\bar{J}$ changes from 18 to 24 when C is changed from ∞ to $B/2$.

In the discussion on the peak at $J=0$, the crucial point is the probability of $\Delta J_r=0$ transitions for the perturbing molecule. As a consequence, in the case of broadening by a symmetric top foreign gas, the presence of the peak depends on the value of the rotational constant C of the perturbing molecule, not of the absorbing molecule.

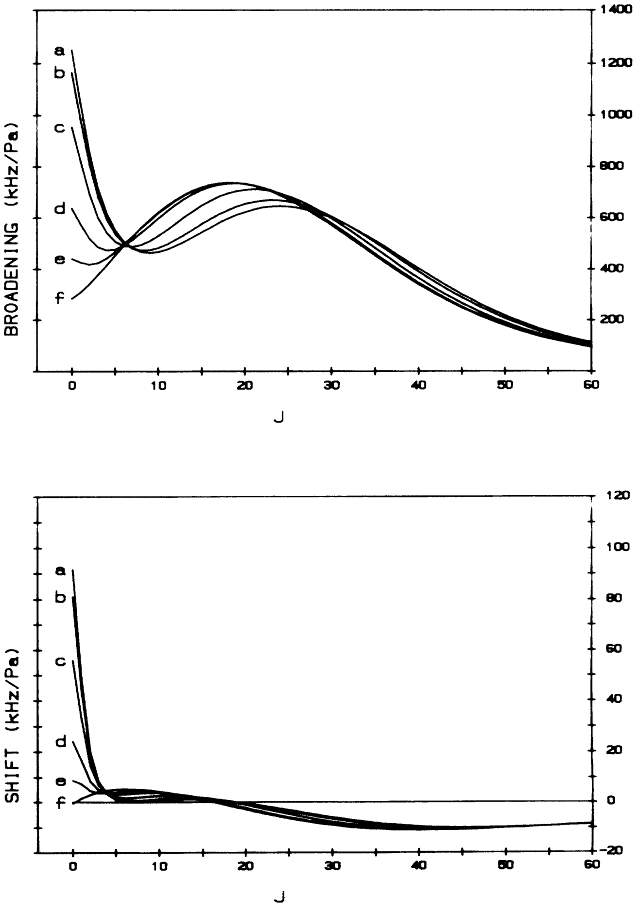

FIG. 6. Variation of the J dependence of broadening and shift parameters with the rotational constant C. The six curves represent the following cases: (a) $C=B/2 \simeq 0.15$ cm^{-1}, a near oblate symmetric top; (b) $C=B \simeq 0.3$ cm^{-1}, a spherical top; (c) $C=1$ cm^{-1}; (d) $C=4.94$ cm^{-1}, the true value for CH_3CN; (e) $C=20$ cm^{-1}; (f) $C=\infty$, a linear molecule.

As far as the dependence of broadening and shift on the quantum number K is concerned, we note that in Eqs. (10) and (11) the k arguments of the resonance functions are essentially independent of K so that the K dependence is restricted to the Clebsch-Gordan coefficients. The coefficient involved in $\Delta J = 0$ transitions is $\sim K^2/J^2$, while that for J-changing transition is $\sim 1 - K^2/J^2$. Since the broadening effect of the $\Delta J = 0$ transitions is reduced by the middle term, the broadening coefficient is expected to decrease as K increases. However, if we restrict ourselves to low K/J values, the broadening coefficient is expected to be only weakly dependent on K.

IV. DISCUSSION

The effect of interactions other than dipole-dipole interaction was omitted in the qualitative discussion of Sec. III, but, unlike microwave case, it must be taken into account for the FIR lines. Indeed, assuming [17] an electric quadrupole moment of 0.18 ± 0.12D nm for the CH_3CN molecule, the dipole-quadrupole contribution to line-broadening parameters is less than 0.5% for the microwave case but can be as large as 10% for the FIR lines. Unfortunately, the value of the quadrupole moment is not accurately determined, which makes the consideration of contributions from higher-order interactions useless. Another small difference with respect to the calculations for the microwave lines [5] is given by the influence of the hyperfine structure, which can be omitted in the present FIR data because it is unresolved.

The theoretical curves for the J dependence reported in Fig. 4 were performed assuming $T = 296$ K and $K = 0$, and included dipole-quadrupole and quadrupole-quadrupole interactions. Indeed, variations with K of the calculated parameters at fixed J are very small. For $J'' \leq 80$ and $K \leq J''/4$, they are less than 2% for the broadening and less than 2 kHz/Pa for the shift.

The general agreement between theory and experiment is satisfactory if we consider both the approximate character of the theory and the experimental errors. All of the features predicted by the theory are confirmed by the measurements; of particular interest is the experimental confirmation of the absorber-perturber resonance effect. The resonance effect produces important consequences on the temperature variations of the broadening and shift parameters. For the pressure-broadening coefficient $a = w/n$, a power-law temperature dependence is commonly used [18]:

$$a \propto T^{\beta} . \tag{15}$$

The exponent β is usually assumed to range between -1 and -0.5. Indeed, the value $\beta = -1$ can be derived, for a dipole-dipole interaction, if we neglect in Eq. (10) the variations of k produced by changes in the velocity distribution. Within the same approximations it can be shown that $-1 \leq \beta \leq -0.5$ for higher-order interactions.

When we take into account the temperature dependence of the resonance functions, we reach different conclusions. The power law in Eq. (15) turns out to be a rough approximation, valid only within a small temperature range. In the range $T = 256$ to 336 K we have calculated the exponent β for rotational lines with $K = 0$ and J'' ranging from 0 to 80. The results are shown in Fig. 7. The variation of β with J is very large: for the FIR lines, β can even be of opposite sign than for the microwave lines. This can be understood by considering that for $J > \bar{J}$, increasing temperature means a higher population for states of perturbing molecules with $J_r \simeq J_i$ and $J_r \simeq J_f$ and hence an increase of the resonance effect.

Returning to Fig. 4, even though the general features of the theoretical predictions are confirmed by the measurements, discrepancies appear. For lines having large broadening parameters, the calculated values are $\sim$15%–20% too large; for the narrower lines at high J, this discrepancy disappears. The theoretical overestimation of the broadening parameter for J ranging from 0 to $\sim$40 is probably explained by the lowest-order perturbative expansion involved in the ATC approximation. The first omitted term (fourth order), although difficult to calculate accurately, is negative.

The decrease of the calculated broadening parameter at higher J is connected with the decreasing probability of adiabatic and resonant collisions (yielding a high value for the resonance function) and an increasing importance of collisions with larger amounts of energy transferred between translation and rotation. Hence, the better agreement at high J is probably due to the fortuitous balance of two opposite errors in the calculations: overestimation due to the lowest-order perturbative expansion and underestimation due to an overly rapid decrease of the f_{dd} resonance function.

On the whole, the fact that the calculated high J decrease of the broadening parameter is faster than the experimental decrease seems to indicate that an improvement of the ATC theory should be obtained by imposing on the resonance function $f_{dd}(k)$ a less rapid decrease at high K. This supposition is confirmed by a recent study on the rovibrational ammonia spectrum [19], suggesting that for that dipolar molecule, ATC calculations could also be affected by a small overestimation of the broadening contributions from adiabatic or resonant collisions and a small underestimation of the contribution from

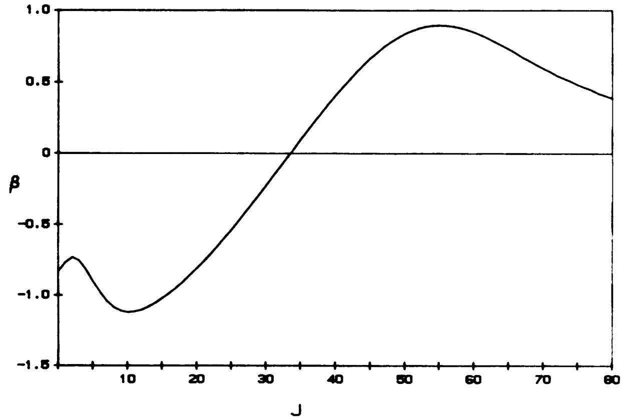

FIG. 7. Theoretical variation of the pressure-broadening temperature exponent β with J.

strongly diabatic transitions. However, more experimental studies are needed before firm conclusions can be made on this point. A possible test of our hypothesis is an accurate measurement of the temperature dependence on J, which, if we are right, should be a little less pronounced than that shown in Fig. 7.

V. CONCLUSIONS

We have measured self-pressure-broadening and shift for 11 rotational transitions in CH_3CN, ranging in frequency from 0.4 to 1.2 THz. The broadening parameter was determined within 10% in most cases, and the shift was determined to only about 40% accuracy. Measurements of transitions with the same J values but different K values showed slight differences in the broadening and shift, but these changes are well within the experimental error.

The data are clear evidence of the large effect of absorber-perturber resonance. This gives rise to a J-dependent maximum in the pressure broadening near $J''=\bar{J}$ (the most populated rotational level). Also, the value of the frequency shift changes sign depending on the sign of $\bar{J}-J''$. Both of these effects are qualitatively confirmed by the theory; quantitative differences indicate improvements and corrections that need to be considered in the theory.

ACKNOWLEDGMENTS

This work was supported in part by a contribution from the U.S. Government and in part by NASA Grant No. W-15,047.

[1] W. R. MacGillivray, J. Phys. B **9**, 2511 (1976).

[2] H. Mäder, H. Bomsdorf, and U. Andresen, Z. Naturforsch., Teil A **34**, 850 (1979).

[3] G. Buffa, A. Di Lieto, P. Minguzzi, and M. Tonelli, Int. J. Infrared Millimeter Waves **2**, 559 (1981).

[4] J. Haekel and H. Mäder, J. Quant. Spectrosc. Radiat. Transfer **41**, 9 (1989).

[5] G. Buffa, D. Giulietti, M. Lucchesi, M. Martinelli, and O. Tarrini, J. Chem. Phys. **90**, 6881 (1989) and references therein.

[6] D. Derozier and F. Rohart, J. Mol. Spectrosc. **140**, 1 (1990).

[7] I. J. Nolt, K. V. Chance, L. R. Zink, D. A. Jennings, K. M. Evenson, M. D. Vanek, and J. V. Radostitz, Eleventh International Conference on Infrared and Millimeter Waves, Conference Digest, edited by G. Moruzzi (ETS Editrice, Pisa, Italy, 1986), pp. 286–288; K. M. Evenson, D. A. Jennings, L. R. Zink, and M. Inguscio, *ibid.*, pp. 98–100.

[8] P. W. Anderson, Phys. Rev. **76**, 647 (1949).

[9] C. T. Tsao and I. Curnutte, J. Quant. Spectrosc. Radiat. Transfer **2**, 41 (1962).

[10] K. M. Evenson, D. A. Jennings, and M. D. Vanek, in *Frontiers in Laser Spectroscopy of Gases*, edited by A. C. P. Alves, J. M. Brown, and J. M. Hollas (Kluwer, Dordrecht, The Netherlands, 1988), pp. 43–51.

[11] L. R. Zink, P. De Natale, F. S. Pavone, M. Prevedelli, K. M. Evenson, and M. Inguscio, J. Mol. Spectrosc. **143**, 304 (1990).

[12] E. N. Grossman, Infrared Phys. **29**, 875 (1989).

[13] G. W. Schwaab, D. Galleguillos, R. Wattenbach, and H. P. Röser, Fourth International Conference on Infrared Physics, Conference Proceedings, Zürich, 1988, edited by R. Kesserling and F. K. Kneubühl (unpublished), pp. 513–515.

[14] G. W. Schwaab, Ph.D. thesis, Universität Bonn, 1990 (unpublished); G. W. Schwaab, K. M. Evenson, and L. R. Zink (unpublished).

[15] G. Buffa and O. Tarrini, Appl. Opt. **28**, 1800 (1989) and references therein.

[16] A. S. Pine and A. Fried, J. Mol. Spectrosc. **114**, 148 (1985).

[17] J. N. Pochan, R. L. Shoemaker, R. G. Stone, and W. H. Flygare, J. Chem. Phys. **52**, 2478 (1970).

[18] C. H. Townes and A. L. Schawlow, Microwave Spectroscopy (Dover, New York, 1955), pp. 368–369.

[19] G. Baldacchini, G. Buffa, and O. Tarrini, Nuovo Cimento D **13**, 719 (1991).